J. Anat. (1999) **195**, pp. 587–604, with 26 figures Printed in Great Britain

The vomeronasal organ of the South American armadillo *Chaetophractus villosus* (Xenarthra, Mammalia): anatomy, histology and ultrastructure

P. D. CARMANCHAHI[1], H. J. ALDANA MARCOS[1,2], C. C. FERRARI[1] AND J. M. AFFANNI[1,2]

[1] *Institute of Neurosciences, University of Buenos Aires, Buenos Aires, and* [2] *Faculty of Medicine, University of Morón, Morón, Argentina*

(*Accepted 7 July 1999*)

ABSTRACT

The vomeronasal organ (VNO) is a chemoreceptive structure that has not been extensively studied in the Xenarthran order. Tissue samples from the VNO of the armadillo *Chaetophractus villosus* were prepared for light and electron microscopy. The VNO is located in the anterior part of the base of the nasal septum. It is tubular in shape, $\sim$ 18 mm in length and opens in the rostral region of the nasal cavity and with a blind caudal end. Its lumen is lined by sensory (SE) and nonsensory (NSE) epithelium. The SE shows sensory, supporting and basal cells whereas the NSE contains ciliated and nonciliated secretory cells and basal cells. At the ultrastructural level, the sensory cells appear as bipolar neurons with conspicuous microvilli on their free surface. The supporting cells of the SE contain numerous membrane-bound vesicles in their apical regions. A peculiar feature not found in other mammals, is the presence of concentric whorls of RER cisterns frequently observed in their basal expansions. Infiltrating plasma cells can be detected in the SE basal region close to the dorsal junctional area. This region also exhibits an unusual type of basal cell, probably responsible for the generation of new vomeronasal receptor neurons. The ciliated NSE cells exhibit numerous ovoids or irregularly shaped membranous protrusions projecting from the plasma membrane of the cilia. As far as we know, this is the first study reporting the presence of this feature in ciliated NSE cells. The nonciliated cells are characterised by scarce large secretory granules and apical microvilli. The vomeronasal glands are compound-branched tubuloacinar glands with serous acinar cells. Four types of secretory granules are present. The ducts of these glands reach the lumen in the dorsolateral region between the NSE and SE. Hypolemmal nerve terminals were observed contacting secretory cells. Fenestrated and nonfenestrated capillaries constitute the vascular supply to these glands. Plasma cells, intimately associated with acinar cells, were frequently observed.

Key words: Olfaction; chemoreception; Jacobson's organ; vomeronasal glands.

INTRODUCTION

The vomeronasal organ (VNO) is a tubular organ situated bilaterally at the base of the nasal septum. Its lumen is lined by 2 different epithelia, sensory and nonsensory, in most species (Eisthen, 1992). Communication either with the nasal or the oral cavities or both may be found (Estes, 1972). The VNO occurs in most terrestrial vertebrates (Døving & Trotier, 1998). It plays an important role in reproductive physiology and sexual behaviour (Halpern, 1987). Rather surprising findings have been reported for the human VNO. This organ has long been considered as vestigial or nonfunctional (Meredith, 1991). However, it was recently characterised as a functional organ capable of eliciting autonomic, endocrine and electroencephalographic (EEG) responses (Moran et al. 1995).

The species of the Xenarthra order retain some primitive mammalian characters and lack the derived features found in other placental mammals. In

Correspondence to Dr Pablo D. Carmanchahi, Instituto de Neurociencia (CONICET), FCEyN, Ciudad Universitaria, Pab. II, 4 piso. Lab. 102, (1428) Buenos Aires, Argentina. e-mail: pdc@bg.fcen.uba.ar

addition, molecular studies indicate that xenarthrans diverged from other eutherians simultaneously with the marsupial–eutherian separation (Engelmann, 1985; Novacek, 1994). These findings suggest that xenarthrans represent a sister group to all other placental mammals (McKenna, 1975).

Neuroanatomical studies performed in our Institute on the armadillo *Chaetophractus villosus* have described highly developed nasal structures (Ferrari, 1997), main and accessory olfactory bulbs, and related brain regions (Benítez et al. 1994). Furthermore, in this armadillo, the VNO has been found to play a role in the regulation of electrical activity of the olfactory bulb during slow and paradoxical sleep (Affanni & García Samartino, 1984). As a consequence of these findings, a detailed morphological study of the armadillo's VNO appeared potentially rewarding. The presence of VNO in these animals was reported by Broom (1897) and Giancomini (cited in Pearlman, 1934). The structure and ultrastructure of this organ has not been studied in armadillos or in other Xenarthra (sloths and anteaters). The aim of this paper is to describe the structural and ultrastuctural features of the VNO in the South American armadillo *Chaetophractus villosus*.

MATERIAL AND METHODS

Sixteen adult armadillos *Chaetophractus villosus* (8 females, 8 males) were used. The animals were maintained under standard laboratory conditions (light/dark cycle of 12 h; temperature 21 °C; pellet food and water ad libitum). They were anaesthetised with ketamine hydrochloride (40 mg/kg, i.m.) and sodium thiopental (60 mg/kg, i.p.) and killed during spring, summer, autumn and winter. For light microscopic studies the animals were perfused via the aorta with saline solution followed by Bouin's fluid or neutral buffered saline formalin. In order to determine the relative localisation of the VNO, some noses were decalcified in buffered formic acid (Sheehan & Hrapchak, 1980) for 25 d and washed in water for 12 h. In other animals both VNO were removed under a dissecting microscope. The tisues were dehydrated and embedded in paraffin. Serial sagittal and transverse sections (5–8 μm) were stained either with haematoxylin and eosin or Masson's trichrome. For electron microscopy the anaesthetised animals were perfused via the aorta with modified saline (0.8% NaCl, 0.8% sucrose, 0.4% glucose) followed by 2% glutaraldehyde fixative in 0.05 M phosphate buffer, pH 7.2. The specimens were then immersed in the same fixative at room temperature for 2–3 h. The tissues were stored overnight in buffer with 30% sucrose. After 5 min washes in buffer (× 3), they were postfixed in 1% OsO_4 in the same buffer at pH 7.2 for 1 h, washed again, dehydrated in an ethanol series, cleared in acetone, and embedded in Araldite. Semithin (~ 1 μm) and ultrathin sections (~ 0.07 μm) were cut on a Sorvall Porter–Blum ultramicrotome and stained with toluidine blue or contrasted with uranyl acetate and lead citrate, respectively. Ultrathin sections were examined in a Zeiss M-109 Turbo electron microscope. Low power photographs were taken by a contact method, which does not require the use of a photographic camera or microscope (Carmanchahi et al. 1998).

RESULTS

Position and morphology

The VNO of *Chaetophractus villosus* is a paired structure situated under the vomeral bone of the palate. Each organ appears as a hollow cylinder, located bilaterally at the base of the nasal septum (Fig. 1). The length of each VNO was 18 ± 0.41 S.D. mm (n = 8). It communicates rostrally with the nasal cavity through a duct, the incisive canal (Fig. 2), whereas caudally the tube ends blindly. The incisive canals open through pits that are located on the floor of the nasal cavity ~ 1 cm caudal to the tip of the nose. The pits are oval-shaped with a maximum anteroposterior length of 2 mm. The VNO is partially enclosed by a J-shaped hyaline vomeronasal cartilage, which appears incomplete in its dorsolateral region (Fig. 3*a*). Large vascular sinuses, nerves and glandular tissue penetrate into the organ through that region (Fig. 3*a*). The lumen is crescent-shaped in coronal section and is lined with SE and nonsensory NSE (Fig. 3*a*). Additionally, 2 types of junctional area can be defined, one dorsal and other ventrally located. The dorsal one is related to the end of the vomeronasal gland ducts. Both areas show an abrupt transition between SE and NSE. Structural differences were not observed between males and females.

Microscopic description

Epithelia

The incisive canal that provides communication for the VNO with the nasal cavity (Fig. 2) is covered by stratified squamous epithelium. This epithelium is

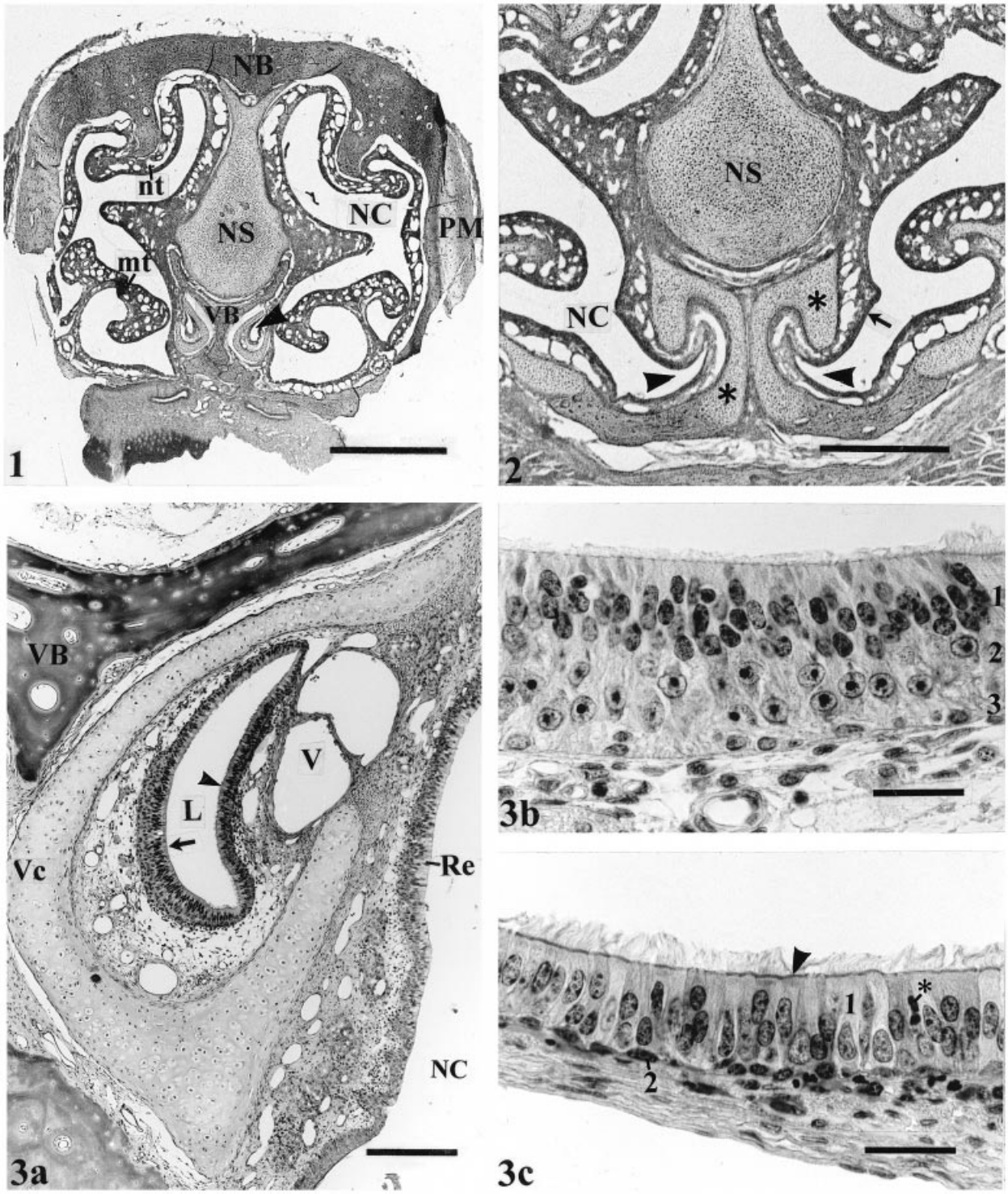

Fig. 1. Low power view of coronal section of nasal cavity of *Chaetophractus villosus*. mt, maxilloturbinate; NB, nasal bone; NC, nasal cavity; NS, nasal septum; nt, nasoturbinate; PM, premaxilla; VB, vomer; arrowhead, vomeronasal organ. Bar, 2.5 mm.

Fig. 2. Low power view showing rostral end of the VNO and its communication with the nasal cavity (arrowheads). NC, nasal cavity; NS, nasal septum; *, vomeronasal cartilage; arrow, respiratory epithelium. Bar, 1.5 mm.

Fig. 3. (*a*) Cross section of middle region of vomeronasal organ of *Chaetophractus villosus*. Masson trichrome. L, lumen of the VNO; NC, nasal cavity; Re, respiratory epithelium; VB, vomeronasal bone; Vc, vomeronasal cartilage; V, large vascular sinuses; arrow, sensory epithelium; arrowhead, nonsensory epithelium. Bar, 200 μm. (*b*) Vomeronasal sensory epithelium with 3 distinct layers: 1, supporting cells; 2, vomeronasal receptor neurons; 3, basal cells. Haematoxylin and eosin. Bar, 30 μm. (*c*) Vomeronasal nonsensory epithelium. Only ciliated cells (1) and basal cells (2) can be distinguished at light microscopic level. Note the conspicuous line of basal bodies (arrowhead) and migrating cell (*). Haematoxylin and eosin. Bar, 30 μm.

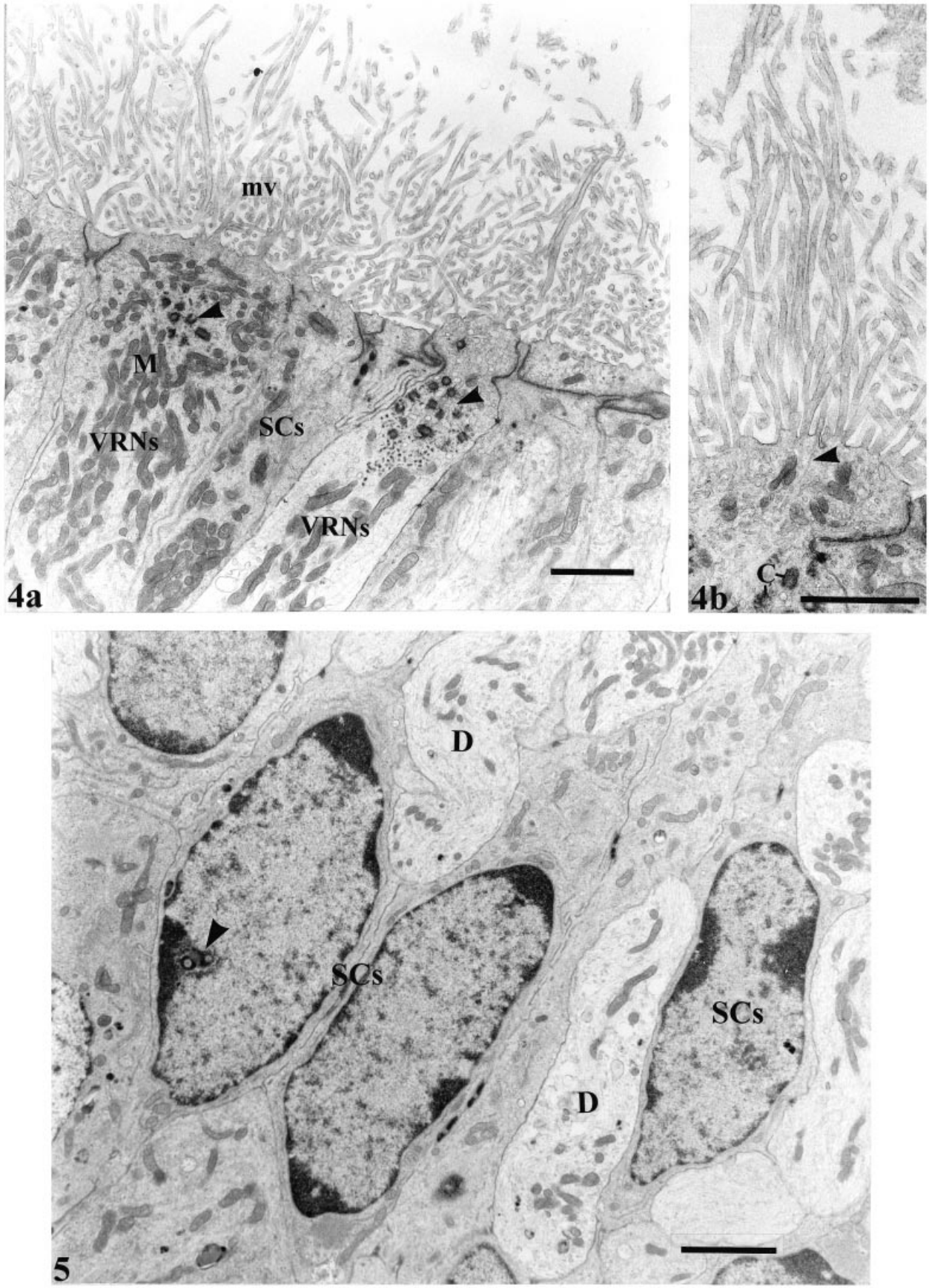

Fig. 4. (*a*) Apical region of the SE of *Chaetophractus villosus* showing the vomeronasal receptor neurons (VRNs) between supporting cells (SCs). mv, microvilli; M, mitochondria. Note the long microvilli on the free surface of both types of cell and the clumps of centrioles

replaced caudally by the one characteristic for the organ.

Sensory epithelium. The SE is a 75–85 μm high pseudostratified epithelium containing 3 morphologically identifiable cell layers: supporting cells (SCs), vomeronasal receptor neurons (VRNs) and basal cells (BCs) (Fig. 3*b*).

The SCs form a discrete and conspicuous columnar layer in the outer region of the SE, extending from the basal membrane to the epithelial surface. The nuclear region is situated in the apical extremity (Fig. 3*b*). The apical surface is covered by numerous microvilli which are occasionally branched (Fig. 4*a*, *b*). The supranuclear cytoplasm contains many tubular mitochondria, pinocytotic vesicles, numerous membrane-bound vesicles, multivesicular bodies, scarce rough and smooth endoplasmic reticulum (RER and SER) and free ribosomes (Fig. 4*a*). Junctional complexes indicate the close relationship between VRNs and SCs as well as between neighbouring SCs (Fig. 4*a*). The perinuclear cytoplasm contains SER, Golgi complexes, microtubules and numerous longitudinally oriented tubular mitochondria (Fig. 5). The nuclei are ovoid and slightly irregular with clumps of peripheral heterochromatin. A conspicuous nucleolus can also be observed (Fig. 5). The infranuclear cytoplasm narrows into a process that runs towards the basal region, between VRN cell bodies. These processes end in basal expansions, which lie on the basal membrane (Fig. 8*a*). They appear to be joined by means of desmosomes and contain mitochondria, lipofuscin granules, and free ribosomes. Concentric whorls of RER cisterns are frequently observed (Fig. 8*a*).

The VRNs are bipolar cells. The nuclear region is usually situated below the nuclear level of the SC (Fig. 3*b*). The perikaryon is frequently observed contacting other VRNs or with basal expansions of SCs (Fig. 6). A peripheral dendritic process extends from the cell body towards the epithelial surface, whereas a central axon goes towards the basal lamina. The dendrite runs between the nuclei of SCs before expanding into a region that ends in a rounded ending carrying numerous microvilli (Figs 4*a*, 5, 7*a*). The microvilli are long (4.94 ± 0.48 S.D. μm; $n = 5$), either branched or not and contain a fibrillar core with a longitudinal arrangement extending into the apical cytoplasm (Figs 4*a*, 7*a*). A thin glycocalyx covering the microvilli can also be seen. Dendrites are easily distinguished from the surrounding SCs by their electron-lucent cytoplasm with SER, pinocytotic vesicles, tubular mictochondria, small clear vesicles, clumps of centrioles and longitudinally oriented microtubules (Figs 4*a*, 5). The apical region of dendrites shows clumps of centrioles associated with striated rootlet fibres, which appear as a striated bundle of filaments, and basal feet extending radially from the basal corpuscle (Fig. 7*a*). The supranuclear cytoplasm is characterised by highly developed Golgi complexes, RER, SER, secondary lysosome-like bodies, numerous lipofuscin granules, multivesicular bodies and tubular mitochondria (Fig. 6). The pale nucleus appears rounded, with an irregular perinuclear membrane and scanty peripheral chromatin. An enormous central heterochromatin block appears associated with 1 or 2 nucleoli (Figs 6, 7*b*). Both perinuclear and infranuclear cytoplasm shows abundant RER, multivesicular bodies, lipofuscin granules, tubular mitochondria, lysosome-like bodies and free ribosomes (Figs 6, 8*a*).

BCs are confined to a conspicuous layer of cells intimately associated with the basal membrane (Fig. 3*b*). They are irregularly shaped with the long axis parallel to the basal lamina (Fig. 8*a*). Both cytoplasm and nucleus are slightly electron dense. The nuclei are oval or round with a thin rim of peripheral chromatin and heterochromatin clumps scattered throughout the karyoplasm (Fig. 8*a*). A nucleolus is frequently observed. The cytoplasm contains free ribosomes, RER, vesicles, small Golgi complexes and mitochondria (Fig. 8*a*, *b*). Large bundles of tonofilaments are often seen (Fig. 8*b*). Desmosomes are found between BCs and neighbouring cells (Fig. 8*b*). Hemidesmosomes link BCs to the basal lamina (Fig. 8*b*). Axons of the VRNs unensheathed by the cytoplasm of the BCs are observed.

The SE of the junctional area shows 2 types of BC. One is similar to those found in the remaining SE. The second, less frequent, has an ovoid or round profile, large nuclei and scarce cytoplasm. Both nucleus and cytoplasm are electron lucent (Fig. 9). Nucleoli were not seen. The cytoplasm contains numerous free ribosomes and mitochondria but other organelles are scarce. No bundles of tonofilaments are observed (Fig. 9).

Infiltrating plasma cells can be seen in the basal region of the SE close to the dorsal junctional area. They can be observed either with nondilated (Fig.

(arrowhead) in the VRNs. Bar, 0.7 μm. (*b*) Distal end of the dendrite of a VRN. Long microvilli, branched and unbranched, with fibrillar cores (arrowhead) extending within the apical cytoplasm can be seen. C, centrioles. Bar, 0.7 μm.

Fig. 5. Nuclear region of the supporting cells (SCs) with dendrites (D) running between them. Dendrites are easily distinguished from the surrounding SCs by their electron lucent cytoplasm. Arrowhead, nucleolus. Bar, 0.2 μm.

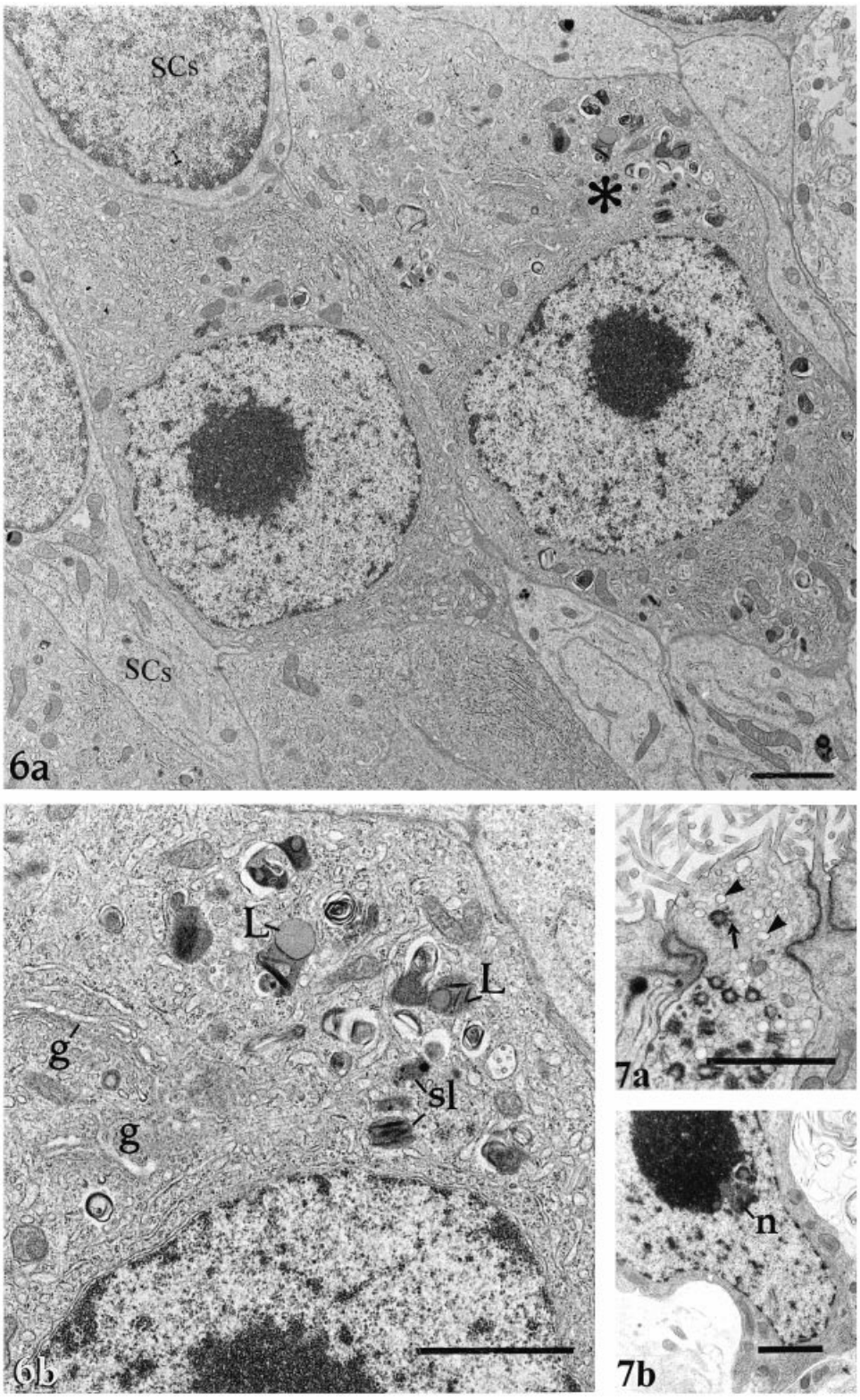

Fig. 6. (*a*) Longitudinal section including the soma of 2 vomeronasal receptor neurons. The nucleus of the neuron is characterised by a large central heterochromatin block and scanty peripheral chromatin. The perinuclear cytoplasm contains large amounts of RER, secondary lysosome-like bodies and lipofuscin granules. SCs, supporting cells. Bar, 0.7 μm. (*b*) Detail of the supranuclear cytoplasm of the neuron labelled with the asterisk in *a* showing several Golgi complexes (g), RER, scattered cisterns of SER; sl, secondary lysosomes-like bodies; L, lipofuscin granules. Bar, 0.7 μm.

Fig. 7. (*a*) Detail of a dendritic process of the VRNs with small clear vesicles (arrowheads) and centrioles with basal foot (arrow). Bar, 0.7 μm. (*b*) Detail of a nucleus of vomeronasal receptor neurons with a central clump of heterochromatin associated with the nucleolus (n). Bar, 0.2 μm.

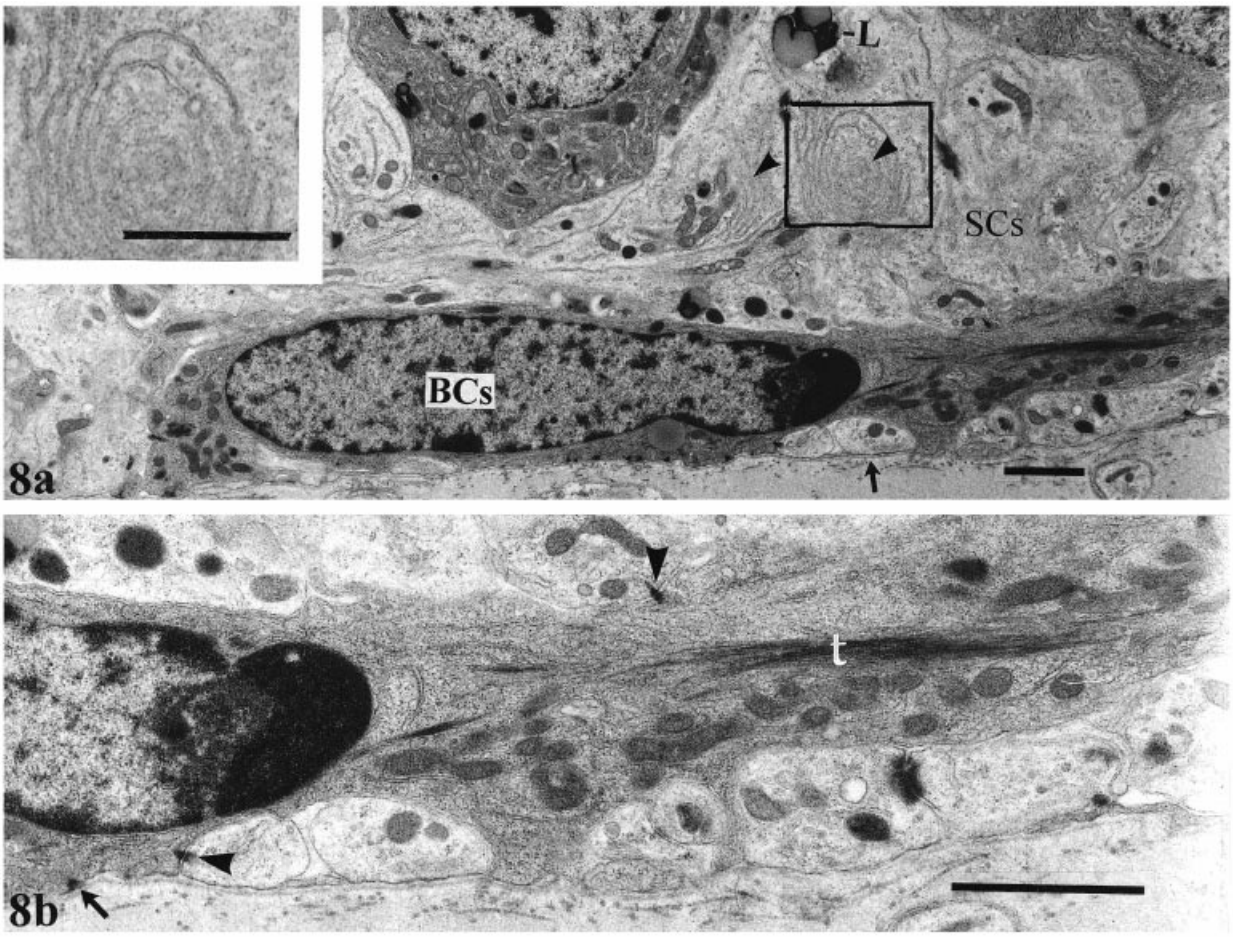

Fig. 8. (*a*) Basal region of sensory epithelium. The flat basal cell (BCs) contacting the basal lamina is characterised by a moderately electron dense cytoplasm and nucleus. The basal expansions of supporting clels (SCs) contact either the BCs or the basal lamina (arrow). Note the presence of tightly packed set of concentric whorls of RER cisterns (arrowheads) and lipofuscin granules (L) in the basal expansions. Bar, 0.7 μm. The inset shows a higher magnification of concentric whorls of RER cisterns marked in the figure. Bar, 0.70 μm. (*b*) Higher magnification of a portion of the basal cell shown in the upper panel. The cytoplasm contains free ribosomes, RER, tubular mitochondria and large bundles of tonofilaments (t). Hemidesmosomes join BCs to the basal lamina (arrow). Desmosomes are present between BCs and neighbouring cells (arrowheads). Bar, 0.7 μm.

10*a*) or dilated (Fig. 10*b*) RER. They are intimately related to the soma and axomal projections of the VRNs and the basal expansions of the SCs (Fig. 10*b*).

Nonsensory epithelium. The NSE is a pseudostratified columnar epithelium with 3 cell types: ciliated cells (CCs), nonciliated secretory cells (SeCs) and basal cells (BCs) (Fig. 3*c*). Infiltrating neutrophils are frequently observed among the epithelial cells (Figs 3*c*, 11).

CCs are columnar with long cilia (8.78 ± 0.29 S.D. μm; $n = 5$). They show regularly oriented and branched microvilli in their apical surfaces (Fig. 12). The cilia are related to a regular row of basal bodies located in the apical region (Figs 3*c*, 12). The internal structure of the cilia shows the typical arrangement of motile cilia. Accessory structures, such as striated rootlet fibres and basal feet can be seen (Fig. 12). Numerous ovoid or irregularly shaped membranous protrusions of different lengths and diameters extend from the ciliary membrane (Figs 12, 13*a*, *b*). The apical cytoplasm shows many tubular mitochondria, REL, small vesicles, glycogen particles (alpha type) and centrioles (Fig. 12). Junctional complexes occur between CCs and SeCs as well as between neighbouring CCs (Fig. 12). The supranuclear cytoplasm contains tubular longitudinally oriented mitochondria, RER, free ribosomes, REL, small lipofuscin granules and Golgi complexes. The nucleus is oval with a thin rim of peripheral heterochromatin. The nucleolus is located close to the inner nuclear membrane (Fig. 11). The infranuclear cytoplasm narrows into a process contacting neighbouring cells by means of desmosomes and reaching the basal membrane (Fig. 11).

SeCs are less frequent than CCs (Fig. 11). Their cytoplasm is thinner and more electron-dense than

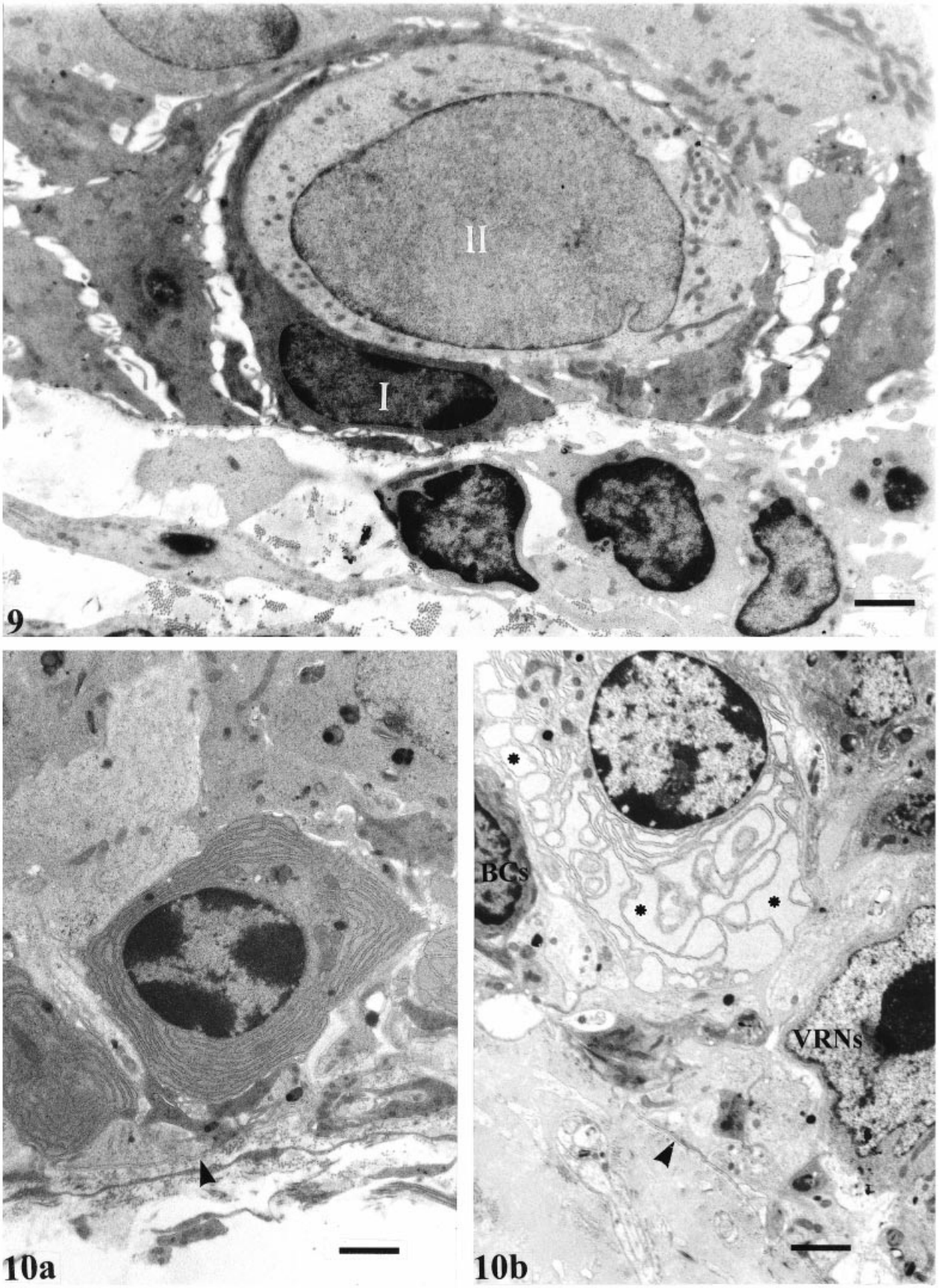

Fig. 9. Basal region of the SE junctional area. Note the presence of 2 types of basal cell. Type I is characterised by a moderately electron dense cytoplasm and nucleus. A type II with pale cytoplasm and nucleus is also seen. Bar, 0.7 μm.

that of CCs (Figs 11, 14*a*). They are characterised by a few large secretory granules and apical microvilli (Fig. 14*b*). In contrast to CCs they are not ciliated (Figs 11, 14*b*). The microvilli show a peculiar arrangement of evenly spaced small spherical particles intimately associated with the glycocalyx (Figs 14*b*, 15). Junctional complexes link adjacent cells (Fig. 14*b*). A dense SER network and abundant mitochondria fill the apical cytoplasm. Large and homogeneous lucent matrix secretory granules were observed in this region (Fig. 14*a*). They are bounded by a single unit membrane (Fig. 14*b*). The discharge of secretory granules may be described as a merocrine mechanism (Fig. 16). The apical region also contains numerous pinocytic vesicles, centrioles, multivesicular bodies, bundles of intermediate filaments, RER and free ribosomes (Figs 14*b*, 16). The supranuclear cytoplasm contains a conspicuous Golgi complex associated with putative secretory granules, a few parallel cisterns of RER, free ribosomes, lipofuscin granules and mitochondria (Fig. 14*a*). The nucleus is ovoid with peripheral heterochromatin clumps and a nucleolus (Fig. 14*a*). The basal region shows free ribosomes and mitochondria. The SeCs are attached to the basal membrane by numerous hemidesmosomes.

BCs show the same ultrastructural characteristics of the BCs described in the SE (Fig. 11). The loosening of cellular contact between the BCs and the basilar expansions of CCs and SeCs results in the enlargement of the intercellular spaces forming a 'basal labyrinth' (Figs 11, 17). Numerous microvilli extend from the BCs and adjacent cells towards the intercellular spaces (Fig. 17). Cellular processes with desmosomes are interposed between the BCs as well as between the basal processes of SeCs and CCs (Fig. 17).

Infiltrating cells with the ultrastructural features of neutrophils are frequently observed in the NSE and in the junctional area between the SE and NSE (Fig. 11). Their relation to neighbouring cells is made by simple contact of opposing membranes or through intercellular spaces.

Lamina propria

The lamina propria that underlies the sensory epithelium is composed of loose connective tissue with abundant ground substance, collagen and reticular fibres. Fibroblasts, macrophages, plasma cells, mast cells and infiltrating leucocytes (mononuclear and polymorphonuclear) can be observed. Fenestrated and nonfenestrated capillaries, as well as lymphatic vessels and small vascular sinuses were distinguishable. Bundles of unmyelinated axons cross the lamina propria and converge on the submucosa, forming the vomeronasal nerve.

The lamina propria under the nonsensory epithelium is characterised by loose connective tissue with a great number of collagen fibres, reticular fibres, scarce ground substance and fewer cells than in the lamina propria under the sensory epithelium. Lymphocytes are the most numerous cells, but a few fibroblasts and plasma cells can also be observed. Large vascular sinuses are spread throughout the lamina propria.

Submucosa

The submucosa shows loose connective tissue with collagen and reticular fibres, fibroblasts, plasma cells, macrophages, large blood vessels, vomeronasal glands (VG) and bundles of vomeronasal nerves. Enormous vascular sinuses (Fig. 3*a*), with a tunica media that comprises 5–7 layers of smooth muscle cells, are present in the region where there is no cartilage. In addition, smaller sinuses are also distributed throughout the submucosa. Both characteristics give the appearance of cavernous tissue to the submucosa.

Vomeronasal glands. The VG are compound-branched tubuloacinar glands mainly located in the submucosa along the long axis of the dorsal aspect of the VNO. Their secretions are released into the lumen of the VNO through ducts ending in the dorsal junctional area. The secretory ducts are lined with simple squamous or cubical epithelium. Junctional complexes join neighbouring cells. The lumen is circular or ovoid in cross section with some stubby microvilli. Some duct cells contain serous-like secretory granules. They show intercellular spaces with microvilli in the laterobasal regions. The glandular endpieces consist of serous acinar cells (Fig. 18). We classify those cells as serous on the basis of their light and electron microscopy appearance (Tandler, 1993; Tandler & Phillips, 1993). They are pyramidal-shaped with round or oval basal nuclei (Fig. 18). The luminal surface is lined by infrequent microvilli. Junctional complexes link adjacent cells (Fig. 18). These cells have all the structural hallmarks of cells geared for synthesis of proteins for export. The supranuclear cytoplasm contains discrete serous-like secretory granules. There are noticeable differences between

Fig. 10. Infiltrated plasma cells in the basal region of the SE junctional area. (*a*) Plasma cells with nondilated RER. Bar, 0.7 μm. (*b*) Plasma cell with dilated RER (*). VRNs, vomeronasal receptor neurons; BCs, basal cells; arrowhead, basal membrane. Bar, 0.7 μm.

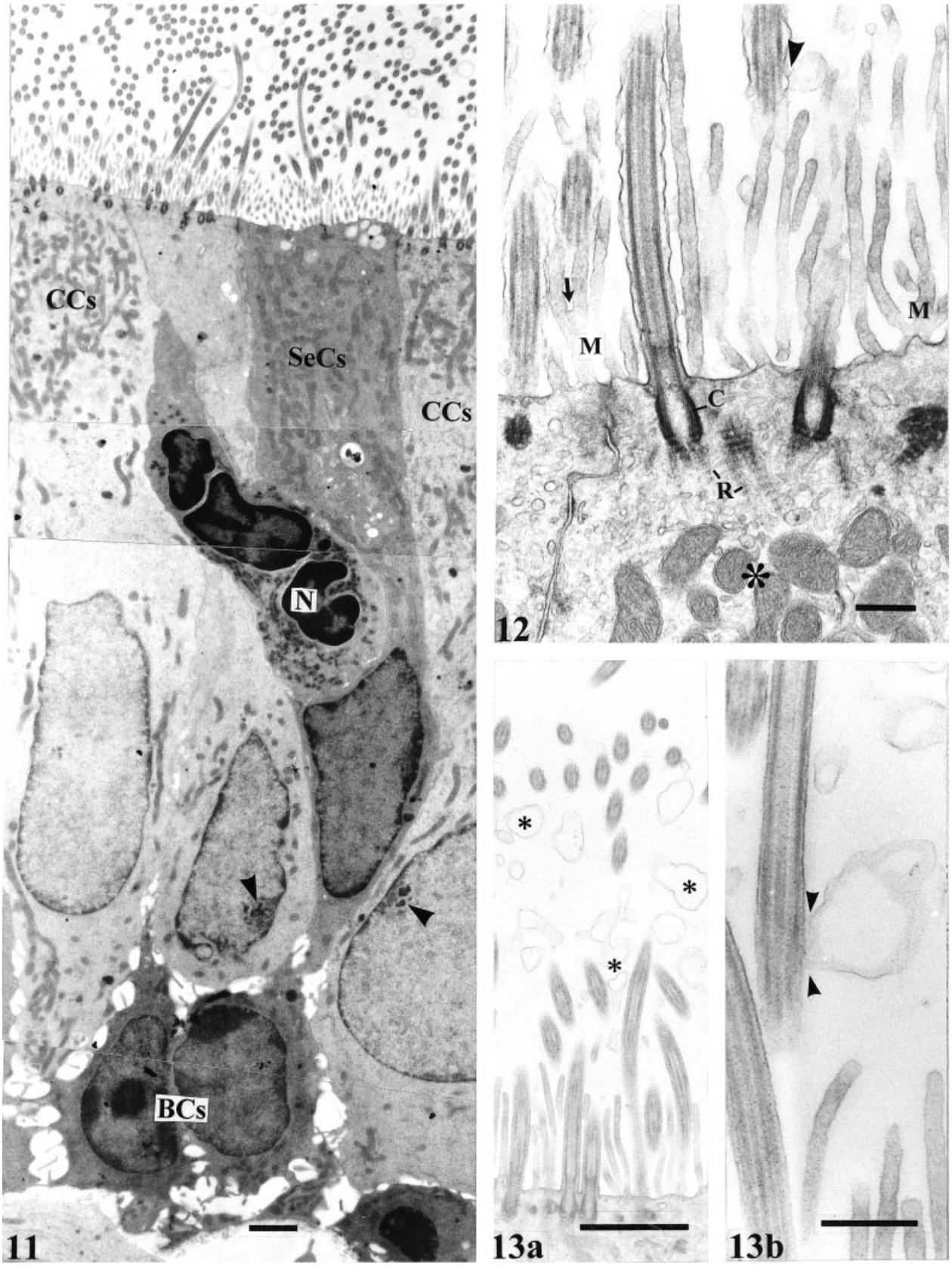

Fig. 11. Nonsensory epithelium of *Chaetophractus villosus* VNO showing ciliated cells (CCs), nonciliated secretory cells (SeCs), basal cells (BCs) and immigrating neutrophils (N). Note intercellular spaces forming a 'basal labyrinth' in the basal region. Arrowhead, nucleolus of CCs. Bar, 0.7 μm.

secretory granules. Four types can be recognized: (1) granules with a homogeneous electron-dense matrix (Fig. 19*a*); (2) granules with a homogeneously electron-dense and structureless matrix in which denser inclusions are suspended (Fig. 19*b*); (3) granules containing a matrix with lucent spherical regions embedded in a material of moderately high density; lenticular inclusions which appear denser than the matrix are also seen (Fig. 19*c*); (4) granules similar to type III without the denser lenticular inclusions (Fig. 19*d*). Their number varies from cell to cell. Some cells have numerous granules almost filling the basal cytoplasm. Others contain only a few granules. Secretory cells without granules are also frequently observed (Fig. 20). The majority of the secretory cells possess type I or type II granules. The mode of discharge of the secretory granules may again be described as merocrine (Figs 20, 22). The Golgi apparatus is mainly seen in apical and middle cytoplasmic regions (Figs 18, 20). The Golgi apparatus of secretory cells with type I granules is associated with putative large low-electron dense secretory granules with a homogeneous matrix (Fig. 21*a*). The Golgi apparatus of secretory cells with type II granules is associated with large putative secretory granules of low electron density in which denser inclusions similar to those of mature granules are seen (Fig. 21*b*). In type III secretory cells, the putative immature secretory granules associated with the Golgi apparatus are ultrastructurally similar to the mature secretory granules but have low electron density (Fig. 21*c*). The different types of secretory granules presumably mature by accretion and compaction of the secretory material. The infranuclear region of the secretory cells shows a tightly packed set of whorl-like RER cisterns between the putative immature secretory granules. The laterobasal regions show intercellular spaces with microvilli (Fig. 22). Mitotic figures were rarely observed in the secretory acini. The basal surfaces of acinar cells directly contact the basal lamina, separating the acinar cells from connective tissue. Myoepithelial cells adjacent to the basal region of the endpieces were not observed. Hypolemmal nerve terminals with numerous clear vesicles and scarce dense-core vesicles adjacent to the basal region of acinar cell come into close contact with glandular cells (Fig. 23). They are usually located in the basolateral intercellular space. A vascular supply with many fenestrated and nonfenestrated capillaries was observed in the interstitial areas of the vomeronasal glands. Plasma cells in intimate contact with acinar cells were frequently observed (Fig. 24).

Vomeronasal nerves. These nonmyelinated nerves are ensheathed by cytoplasmatic processes of Schwann cells branching between the axons (Fig. 25). The Schwann cells show sparse cytoplasm with lipofuscin granules and irregularly shaped nuclei located centrally in the nerve (Fig. 26). Each bundle contains closely packed axons surrounded by basal lamina and collagen fibres forming the endoneurium. The collagen fibres appear longitudinally oriented (Figs 25, 26). The axons possess neurofilaments, microtubules, vesicles and mitochondria (Fig. 26). A thin perineurium encloses each fascicle of nerve fibres (Figs 25, 26). They are composed of a single layer of flattened cells characterised by many pinocytic vesicles. The perineurial cells possess a basal lamina on each side and contact longitudinally oriented collagen fibrils.

DISCUSSION

This study represents the first structural and ultrastructural description of the VNO in the Xenarthra. The VNO of these armadillos opens directly into the nasal cavity. Direct communication has also been observed in the rabbit (Negus, 1958), guinea pig (Negus, 1958), some marsupial species (Estes, 1972), some bat species (Cooper & Bhatnagar, 1976), cat (Ciges & Sánchez, 1977), rat (Vaccarezza et al. 1981), mouse (Taniguchi & Mochizuki, 1983), hamster (Taniguchi & Mochizuki, 1982), chinchilla (Oikawa et al. 1994), man (Moran et al. 1995) and blind mole rat (Zuri et al. 1998).

The armadillo shows SE in the medial wall and NSE in the lateral wall as in most species. In contrast, the NSE is absent in the common marmoset (Taniguchi et al. 1992), man (Moran et al. 1995) and blind mole rats (Zuri et al. 1988).

The fine structure of the receptor cells of the VNO of *Chaetophractus villosus* differs from that of the olfactory receptor neurons (Ferrari et al. 1998). There are no olfactory knobs with cilia. Instead there is a slightly rounded protrusion above the epithelial surface covered with microvilli. Absence of cilia has

Fig. 12. Detail of distal end of 2 ciliated cells of nonsensory epithelium. The cilia exhibit basal bodies (C) and rootlet fibres (R). M, microvilli; arrowhead, membranous protrusion from cilium; arrow, branched microvilli; asterisk, apical accumulation of tubular mitochondria. Bar, 0.7 μm.

Fig. 13. (*a*) Detail of the apical surface of a ciliated cell. Numerous ovoid or irregularly shaped membranous bodies are seen (asterisks). Bar, 0.7 μm. (*b*) Large membranous protrusion extending from the cilium are also visible (arrowheads). Bar, 0.2 μm.

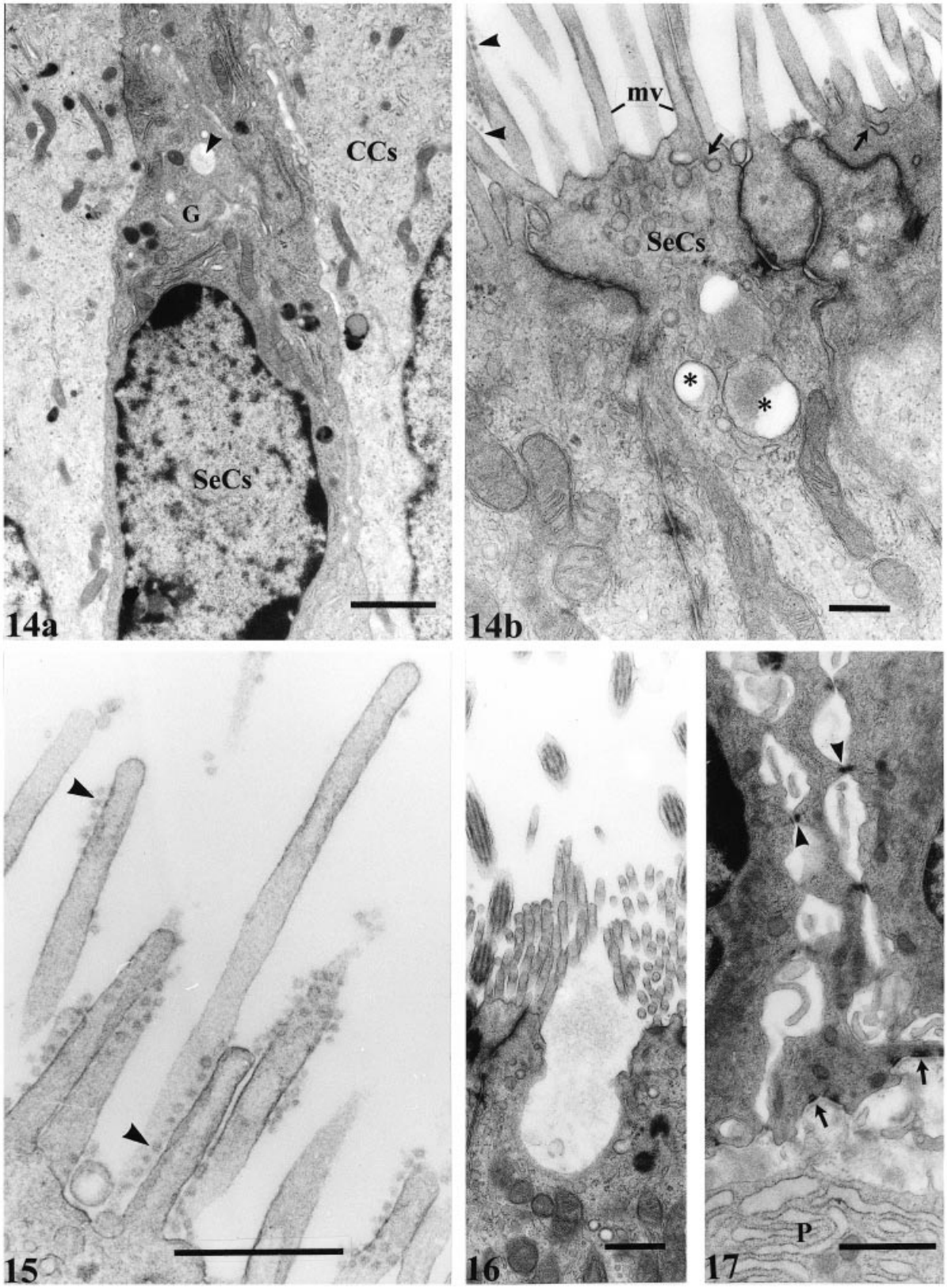

Fig. 14. (*a*) Supranuclear region of nonciliated secretory cell (SeCs). Its cytoplasm is more electrondense than that of ciliated cells (CCs). It contains Golgi complexes (G) associated with putative secretory granules (arrowhead), parallel cisterns of RER, mitochondria and lipofuscin granules. Bar, 0.7 μm. (*b*) Apical region of nonciliated secretory cells (SeCs) bearing numerous microvilli (mv). Notice that the microvilli are partially covered with small spherical particles (arrowheads). Secretory granules (asterisks) and pinocytic vesicles (arrow) are seen. Junctional complexes link neighbouring cells. Bar, 1.4 μm.

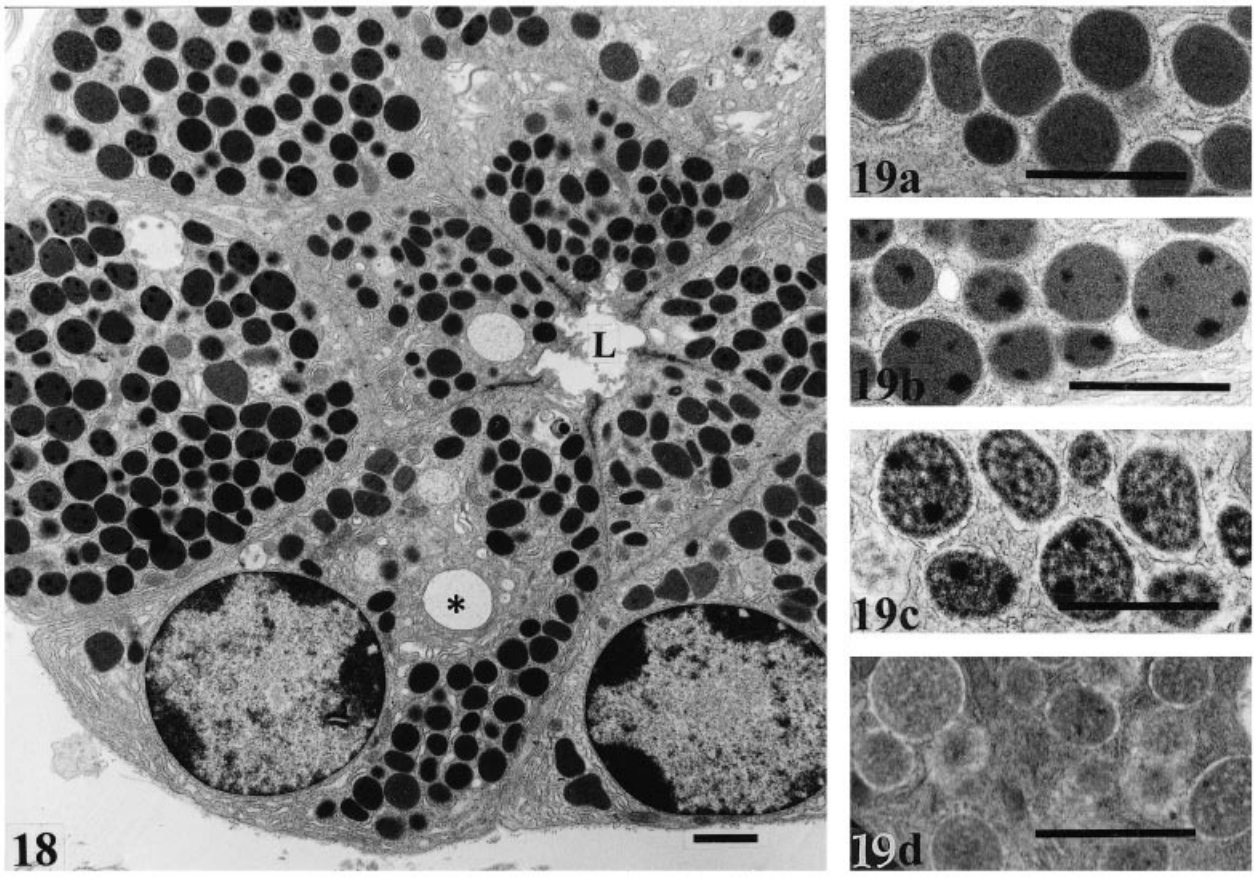

Fig. 18. Secretory cells lining the tubuloacinar secretory endpieces characterised by a basally located round nucleus and numerous serous electron-dense granules. Putative immature secretory granules are located close to the Golgi sacs (asterisk). L, lumen. Bar, 0.7 μm.

Fig. 19. Gallery of serous secretory granules. (*a*) Type I secretory granules. Bar, 0.7 μm. (*b*) Type II secretory granules. Bar, 0.7 μm. (*c*) Type III secretory granules. Bar, 0.7 μm. (*d*) Type IV secretory granules. Bar, 0.7 μm.

been reported in many mammalian species (Adams, 1992). Microvilli have been considered as the first candidate for the site of chemoreception (Miragal et al. 1979).

It is worth noting that the adluminal portion of the armadillo's dendrites contains clusters of centrioles, many mitochondria and clear vesicles. Clusters of centrioles have also been seen in mice (Kolnberger & Altner, 1971), rat (Vaccarezza et al. 1981), rabbit (Luckhaus, 1969), elephant shrew (Kratzing & Woodall, 1988), bats (Bhatnagar et al. 1982), dog (Adams & Wiekamp, 1984), cow (Adams, 1986), horse (Taniguchi & Mikami, 1985) and tree shrew (Loo & Kanagasuntheram, 1972). The precise functional significance of these centrioles remains uncertain. They could represent either an arrested phase in the development of ciliated receptors (Loo & Kanagasuntheram, 1972) or organising centres for microtubules involved in dendritic transport (Adams, 1992). Concentration of mitochondria near the distal end of the dendrite has been described in sheep (Kratzing, 1971), tree shrew and slow loris (Loo & Kanagasuntheram, 1972). The concentration of mitochondria towards the apex of the cells would imply high metabolic activity in this region (Lewis & Dahl, 1995). A profusion of clear vesicles has been described in VRNs of mice (Kolnberger & Altner, 1971), rat (Vaccarezza et al. 1981), rabbit (Luckhaus, 1969), elephant shrew (Kratzing & Woodall, 1988), bat (Bhatnagar et al. 1982), dog (Adams & Wiekamp,

Fig. 15. Detail of microvilli of the nonciliated secretory cells. Arrowheads point to evenly spaced particles on the surface of microvilli. Bar, 0.2 μm.

Fig. 16. Detail of the apical region of a nonciliated secretory cell in the process of granule discharge. Bar, 0.2 μm.

Fig. 17. Basal region of nonsensory epithelium. Basal cells project cytoplasmic processes into the intercellular space. Note presence of desmosomes between them (arrowheads). P, plasma cell in the lamina propria; arrows, hemidesmosome attached to the basal lamina. Bar, 0.2 μm.

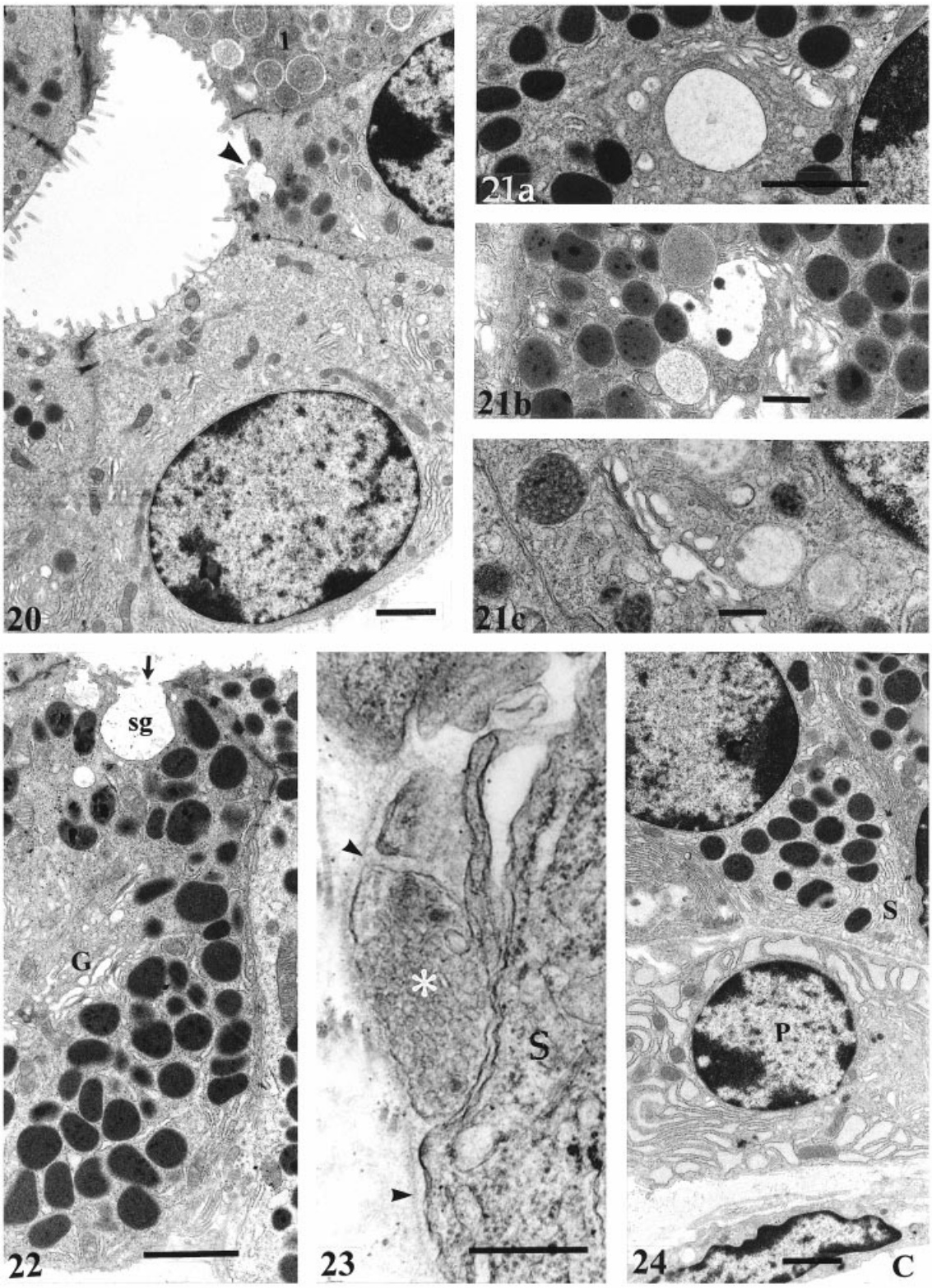

Fig. 20. Abrupt transition from a serous acinar cell on the right towards a cell that has no granules. The arrowhead indicates an invagination produced by exocytosis. A serous acinar cell with secretory granules of the type IV (1) is seen. Bar, 0.7 μm.

Fig. 21. Earliest stages of formation of secretory granules in close relationship to the Golgi apparatus. Bar, 0.2 μm. (*a*) Putative immature type I granule. Bar, 0.20 μm. (*b*) Putative immature type II granule. Bar, 0.2 μm. (*c*) Putative immature type III granules. Bar, 0.2 μm.

Fig. 22. The secretory granule (sg) appears to be secreted from the cell by a merocrine mechanism (arrow). G, Golgi complexes. Bar, 0.7 μm.

Fig. 23. Hypolemmal nerve terminal (asterisk) containing dense-core vesicles and numerous clear vesicles, located near the basal region of secretory cell (S) of vomeronasal glands. Arrowheads, basal lamina. Bar, 0.2 μm.

Fig. 24. Basal region of secretory cells (S) in close relationship to interstitial plasma cell (P). C, capillary. Bar, 0.7 μm.

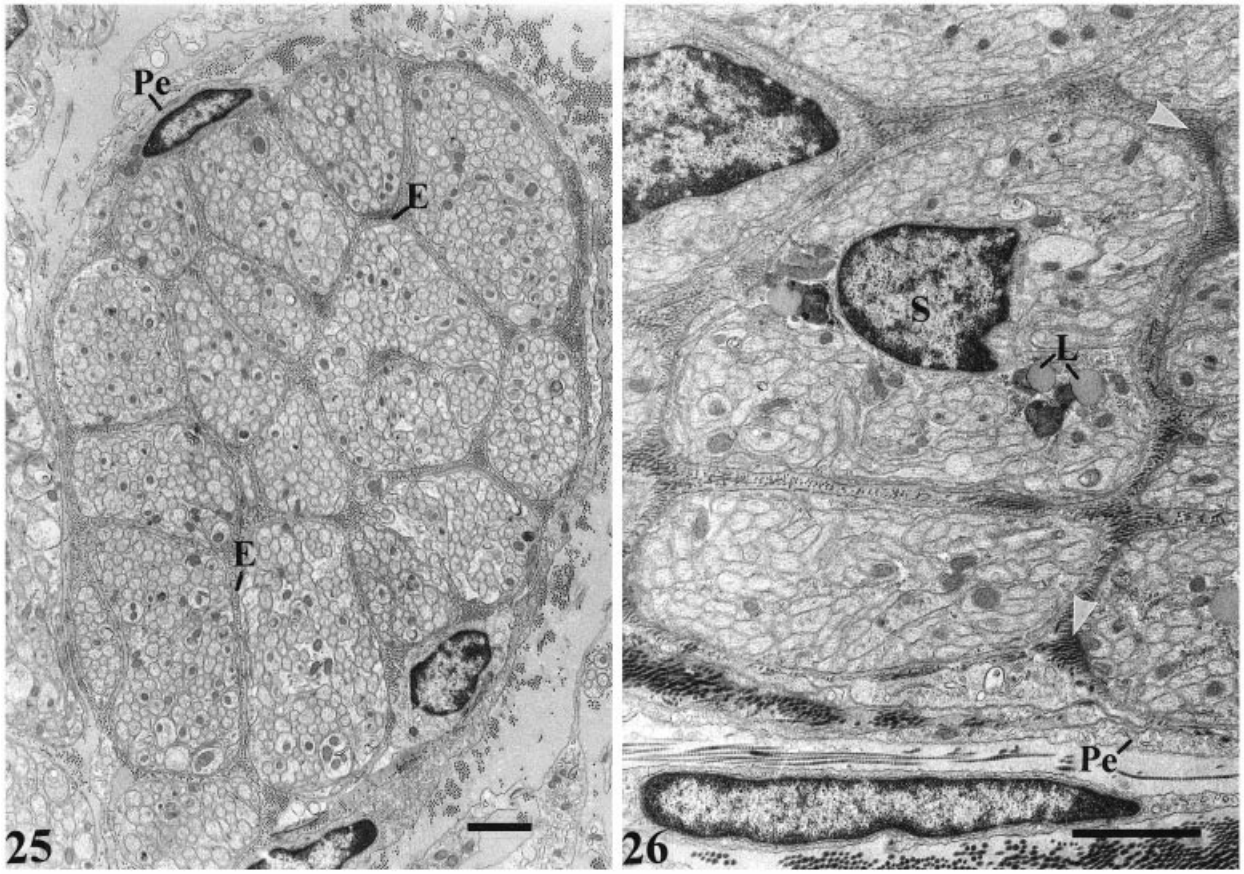

Fig. 25. Transverse section of a fascicle of a vomeronasal nerve composed by 16 compartments containing nerve fibres. Each compartment is composed of unmyelinated axons surrounded by Schwann cells and by collagen fibrils forming the endoneurium (E). The perineurium consists of a single layer of cells (Pe) and associated collagen fibrils. Bar, 0.7 μm.

Fig. 26. Restricted region of the vomeronasal nerve demonstrating the relationship between Schwann cell processes and vomeronasal axons. L, lipofuscin granule; Pe, flattened perineurial cell; S, Schwann cell nucleus; arrowheads, collagen fibrils of the endoneurium. Bar, 0.7 μm.

1984), sheep (Kratzing, 1971), cow (Taniguchi & Mikami, 1985; Adams, 1986) and tree shrew (Loo & Kanagasuntheram, 1972). The presence of these vesicles suggests that this is a highly active endocytotic region where odorant ligand-receptor protein complexes could be internalised (Adams, 1992; Bannister & Dodson, 1992).

In contrast to the findings in most mammals, where the cell bodies contain much SER (Bannister & Dodson, 1992), the armadillo shows numerous RER cisterns. This characteristic is shared with olfactory neurons (Farbman, 1992).

The SCs of armadillos show a peculiar characteristic that differentiates them from those found in other mammals. This feature is the presence of a highly developed RER in the basal processes. The presence of RER in this region could be related to the manufacture of integral membrane proteins or basal exocytosis. However, secretory granules could not be observed in the basal region.

In the SE of our animals, the BCs form a distinct layer that show the same ultrastructural characteristics of flat basal cells found in their olfactory epithelium (Ferrari et al. 1998). Also, BCs with similar characteristics to globose basal cells of the main olfactory epithelium (Ferrari et al. 1998) were found in the SE close to the junctional area. Previous reports identified a population of dividing cells in the junctional area that could give rise to receptor neurons (Barber & Raisman, 1978). On the other hand, in the opossum VNO there is a population of proliferating cells in the basal region close to the basal lamina in the SE (Jia & Halpern, 1998). However, in the armadillo, the role of both types of BCs in neurogenesis needs further analysis.

The occurrence of several cell types in the NSE as seen in the armadillo has also been reported in several mammals (Kratzing, 1971; Loo & Kanagasuntheram, 1972; Ciges & Sánchez, 1977; Adams & Wiekamp, 1984; Taniguchi & Mikami, 1985; Oikawa et al.

1994). An interesting finding in this study is the occurrence of numerous irregularly membranous protrusions of different lengths and diameters protruding from the plasma membranes of the cilia. This may be considered an apocrine type of secretion or a renewal mechanism of the cilia membrane. Nevertheless, the precise functional significance of these remains uncertain. The SeCs of the armadillo show clear signs of secretory activity. The presence of nonciliated cells with apical secretory granules has also been demonstrated in the dog (Adams & Wiekamp, 1984), horse, cattle (Taniguchi & Mikami, 1985) and sheep (Kratzing, 1971). Another remarkable characteristic of the SeCs was the presence of microvilli with a peculiar arrangement of evenly spaced small spherical particles intimately associated with the glycocalyx. These are very similar to the spikes covering the microvilli of the supporting cells in the human olfactory mucosa (Polyzonis et al. 1979).

With respect to the basal region of NSE, *Chaetophractus villosus* shows intercellular spaces joined by desmosomes giving the appearance of a 'basal labyrinth'. Intercellular spaces have been seen in the basal region of dogs (Adams & Wiekamp, 1984), man (Moran et al. 1995) and rats (Vaccarezza et al. 1981). Some authors consider that this region appears to be more sensitive to the osmolality of the solution used during processing than other adjacent tissue (Adams, 1992). We consider that this 'labyrinth' was not an artefact because we used the same treatment for both respiratory and olfactory epithelium and no intercellular spaces were observed in the basal region of these epithelia.

The presence of polymorphonuclear leucocytes in NSE is a common finding in *Chaetophractus villosus*. This feature was also observed in musk shrews (Oikawa et al. 1993), virus-antibody-free rats (Getchell & Kulkarni, 1995), slow loris (Loo & Kanagasuntheram, 1972), rats (Breiphol et al. 1979) and cattle (Adams, 1986). Infiltrating cells have been identified as neutrophils in the VNO in virus-antibody-free rats (Getchell & Kulkarni, 1995). Immunocyte infiltration of the NSE appears to be common among mammals in which the VNO is enclosed in a bony capsule and is organised in such a way that cavernous tissue acts as a pump. Neutrophils provide immune surveillance for the presence of pathogens in the material drawn from the nasal cavity into the VNO and can act as a first line of defence in preventing their invasion of the VNO (Getchell & Kulkarni, 1995).

The architecture of the VG found in the submucosa of *Chaetophractus villosus* was similar to that described in other mammals (Adams, 1992). Only serous acini were found in the armadillo. Serous acini have also been described in prosimian primates (Loo & Kanagasuntheram, 1972), rabbits, guinea pigs, cats, dogs (Ciges & Sánchez, 1977), marsupials (Kratzing, 1984) and mice (Mendoza, 1986). However, mixed mucous and serous VG were described in the hamster (Taniguchi & Mochizuki, 1982), pig (Adams, 1992) and chinchilla (Oikawa et al. 1994).

Four types of serous secretory granules were observed in the armadillo. These may reflect different stages of the secretory cycle or the maturity of individual granules. However, this variability might indicate the presence of different secretions. In accordance with this hypothesis, immature secretory granules similar in texture to the different types of mature granules in the proximity of the Golgi sacs were observed. Different types of electron dense secretory granules have been found in the VG of marsupials (Kratzing, 1984) and in the chinchilla (Oikawa et al. 1994). The secretory granules of the VG differ in structural pattern from the granules described in Bowman's gland in this armadillo (Ferrari et al. 1998), suggesting a different role of these glands in olfactory perception.

The highly developed vascular network and the vast number of fenestrated capillaries in the VG are noteworthy. The presence of fenestrated vessels may indicate endocrine activity by these glands.

The presence of hypolemmal nerve terminals with clear and dense-core vesicles contacting glandular cells in the armadillo suggests participation of the nervous system in the regulation of the secretory activity of the VG. The same type of terminals have also been seen in mice (Mendoza & Kühnel, 1987).

VG have been less studied than the vomeronasal mucosa. However, VG play an important functional role in xenobiotic activity (Rama Krishna et al. 1994), mucous secretion (Cooper & Bhatnagar, 1976), production of possible pheromone-carrier proteins (Ohno et al. 1996) and immunological processes. We assign special importance to the finding of plasma cells intimately associated with both SE and VG. Nasal secretion is known to contain immunoglobulins including IgA and IgM (Getchell & Getchell, 1991). These structures therefore could represent sites of immune secretion towards the lumen of VNO.

The histological and ultrastructural features of the VNO of *Chaetophractus villosus* show that this sensory structure is actively functional in this species. These findings and the presence of a highly developed olfactory mucosa (Ferrari et al. 1998) suggest that the armadillos possess an acute olfactory sense.

ACKNOWLEDGEMENTS

This work was supported by a grant of the Consejo Nacional de Investigaciones Científicas y Técnicas (CONICET). We thank Carina Lopez and Isabel Farias for their excellent technical assistance. The authors also thank LANAIS-MIE (College of Medicine, UBA).

REFERENCES

ADAMS D (1986) The bovine vomeronasal organ. *Archives of Histology of Japan* **49**, 211–225.

ADAMS D (1992) Fine structure of the vomeronasal and septal olfactory epithelia and of glandular structures. *Microscopy Research and Technique* **23**, 86–97.

ADAMS D, WIEKAMP M (1984) The canine vomeronasal organ. *Journal of Anatomy* **138**, 771–787.

AFFANNI JM, GARCIA SAMARTINO L (1984) Comparative study of electrophysiological phenomena in the olfactory bulb of some South American marsupials and edentates. In *Comparative Physiology of Sensory Systems* (ed. Bolis L, Keynes FD, Madrell SHP), pp. 315–331. New York: Cambridge University Press.

BARBER PC, RAISMAN G (1978) Cell division in the vomeronasal organ of the adult mouse. *Brain Research* **141**, 57–66.

BANNISTER L, DODSON H (1992) Endocytic pathways in the olfactory and vomeronasal epithelia in the mouse: ultrastructure and uptake of tracers. *Microscopic Research and Technique* **23**, 128–141.

BENITEZ I, ALDANA MARCOS HJ, AFFANNI JM (1994) The encephalon of *Chaetopractus villosus*. A general view of its most salient features. *Comunicaciones Biológicas* **12**, 57–73.

BHATNAGAR KP, MATULIONIS DH, BREIPOHL W (1982) Fine structure of the vomeronasal neuroepithelium of bats: a comparative study. *Acta Anatomica* **112**, 158–177.

BREIPOHL W, BHATNAGAR KP, MENOZA A (1979) Fine structure of the receptor-free epithelium in the vomeronasal organ of the rat. *Cell and Tissue Research* **200**, 383–395.

BROOM R (1897) A contribution to the comparative anatomy of the mammalian organ of Jacobson. *Transactions of the Royal Society of Edinburgh* **39** (part I), 231–255.

CARMANCHAHI PD, ALDANA MARCOS HJ, FERRARI CC, AFFANNI JM (1998) A simple method for taking photographs of histological sections without using either photographic camera or microscope. *Biocell*. **22**, 207–210.

CIGES M, SANCHEZ G (1977) Ultrastructure of the organ of Jacobson and comparative study with olfactory mucosa. *Acta Otolaryngologica* **83**, 47–58.

COOPER JG, BHATNAGAR KP (1976) Comparative anatomy of the vomeronasal organ complex in bats. *Journal of Anatomy* **122**, 571–601.

DØVING KB, TROTIER D (1998) Structure and function of the vomeronasal organ. *Journal of Experimental Biology* **201**, 2913–2925.

EISTHEN HL (1992) Phylogeny of the vomeronasal system and of receptor cells types in the olfactory and vomeronasal epithelia of vertebrates. *Microscopy Research and Technique* **23**, 1–21.

ENGELMAN G (1985) The phylogeny of the Xenarthra. In *The Ecology and Evolution of Armadillos, Sloths and Vermilinguas* (ed. Montgomery GG), pp. 51–64. Washington D.C.: Smithsonian Institution Press.

ESTES R (1972) The role of the vomeronasal organ in mammalian reproduction. *Mammalia* **36**, 315–341.

FARBMAN AI (1992) Structure of olfactory mucous membrane. In *Cell Biology of Olfaction*, pp. 24–74. Cambridge: Cambridge University Press.

FERRARI CC (1997) The olfactory structure of the armadillos *Chaetophractus villosus* and *Dasypus hybridus*. Doctoral dissertation. Universidad de Buenos Aires, Buenos Aires, Argentina.

FERRARI CC, ALDANA MARCOS HJ, CARMANCHAHI PD, AFFANNI JM (1998) The olfactory mucosa of the south American armadillo *Chaetophractus villosus*: an ultrastructural study. *Anatomical Record* **252**, 325–339.

GETCHELL ML, GETCHELL TV (1991) Immunohistochemical localization of components of the immune barrier in the olfactory mucosa of salamanders and rats. *Anatomical Record* **231**, 358–374.

GETCHELL M, KULKARNI A (1995) Identification of neutrophils in the nonsensory epithelium of the vomeronasal organ in virus-antibody-free rats. *Cell and Tissue Research* **280**, 139–151.

HALPERN M (1987) The organization and function of the vomeronasal system. *Annual Review of Neuroscience* **10**, 325–362.

JIA C, HALPERN M (1998) Neurogenesis and migration of receptor neurons in the vomeronasal sensory epithelium in the opossum, *Monodelphis domestica*. *Journal of Comparative Neurology* **400**, 287–297.

KOLNBERGER I, ALTNER H (1971) Ciliary-structure precursor bodies as stable constituents in the sensory cells of the vomeronasal organ of reptiles and mammals. *Zeitschrift für Zellforschung und mikroskopische Anatomie* **118**, 254–262.

KRATZING J (1971) The structure of the vomeronasal organ in the sheep. *Journal of Anatomy* **108**, 247–260.

KRATZING J (1984) The structure and distribution of nasal glands in four marsupial species. *Journal of Anatomy* **139**, 553–564.

KRATZING J, WOODALL PG (1988) The rostral nasal anatomy of two elephant shrews. *Journal of Anatomy* **157**, 135–143.

LEWIS JL, DAHL AR (1995) Olfactory mucosa: composition, enzymatic localization and metabolism. In *Handbook of Olfaction and Gustation* (ed. Doty R), pp. 33–52. New York: Marcel Dekker.

LOO SK, KANAGASUNTHERAM R (1972) The vomeronasal organ in tree shrew and slow loris. *Journal of Anatomy* **112**, 165–172.

LUCKHAUS VG (1969) Licht und elektronenmikroskopische Befunder an der Lamina epithelialis des Vomeronasalorgans vom Kaninchen. *Anatomischer Anzeiger* **124**, 477–489.

McKENNA MC (1975) Toward a phylogenetic classification of the Mammalia. In *Phylogeny of Primates* (ed. Luckett WP, Szalay FS), pp. 21–46. New York: Plenum Press.

MENDOZA AS (1986) The mouse vomeronasal glands: a light and electron microscopic study. *Chemical Senses* **11**, 541–555.

MENDOZA AS, KUHNEL W (1987) Morphological evidence for a direct innervation of the mouse vomeronasal glands. *Cell and Tissue Research* **247**, 458–459.

MEREDITH M (1991) Sensory processing in the main and accessory olfactory systems: comparison and contrasts. *Journal of Steroid Biochemistry and Molecular Biology* **39**, 601–614.

MIRAGAL F, BREIPOHL W, BHATNAGAR K (1979) Ultrastructural investigation on the cell membranes of the vomeronasal organ in the rat: a freeze-etching study. *Cell and Tissue Research* **227**, 519–534.

MORAN D, MONTI-BLOCH L, STENSAAS L, BERLINER D (1995) Structure and function of the human vomeronasal organ. In *Handbook of Olfaction and Gustation* (ed. Doty R), pp. 793–820. New York: Marcel Dekker.

NEGUS V (1958) *The Comparative Anatomy and Physiology of the Nose and Paranasal Sinuses*, p. 402. London: Livingstone.

NOVACEK MJ (1994) The radiation of placental mammnals. In *Major Features of Vertebrate Evolution. Short Courses in Paleontology* (Randall Spencer Series), pp. 220–237. London: Publications of the Paleontological Society.

OHNO K, KAWASAKI Y, KUBO T, TOHYAMA M (1996) Differential expression of odorant-binding protein genes in rat nasal glands: implication for odorant binding protein as a possible pheromone transporter. *Neuroscience* **71**, 355–366.

OIKAWA T, SHIMAMURA K, SAITO T, TANIGUCHI K (1993) Fine structure of the vomeronasal organ in the house musk shrew (*Suncus murinus*). *Experimental Animal* **42**, 411–419.

OIKAWA T, SHIMAMURA K, SAITO T, TANIGUCHI K (1994) Fine structure of the vomeronasal organ in the chinchilla (*Chinchilla laniger*). *Jikken Dobutsu* **43**, 487–497.

PEARLMAN S (1934) Jacobson's organ (organon vomero-nasale, Jacobsoni): its anatomy, gross, microscopic and comparative, with some observations as well on its function. *Annals of Otology, Rhynology and Laryngology* **43**, 739–768.

POLYZONIS BM, KAFANDARIS PM, GIGIS PI, DEMETRIOU T (1979) An electron microscopic study of human olfactory mucosa. *Journal of Anatomy* **128**, 77–83.

RAMA KRISHNA NS, GETCHELL ML, GETCHELL TV (1994) Expression of the putative pheromone and odorant transporter vomeromodulin mRNA and protein in nasal chemosensory mucosae. *Journal of Neuroscience Research* **39**, 243–259.

SHEEHAN DC, HRAPCHAK BB (1980) Bone. In *Theory and Practice of Histotechnology*, pp. 89–117. London: C. V. Mosby.

TANDLER B (1993) Structure of mucous cells in salivary glands. *Microscopy Research and Techniques* **26**, 49–56.

TANDLER B, PHILLIPS CJ (1993) Structure of serous cells in salivary glands. *Microscopic Research and Techniques* **26**, 32–48.

TANIGUCHI K, MOCHIZUKI K (1982) Morphological studies on the vomeronasal organ in the golden hamster. *Japanese Journal of Veterinary Science* **44**, 419–426.

TANIGUCHI K, MOCHIZUKI K (1983) Comparative morphological studies on the vomeronasal organ in rats, mice and rabbits. *Japanese Journal of Veterinary Science* **45**, 67–76.

TANIGUCHI K, MIKAMI S (1985) Structure of the epithelia of the vomeronasal organ of horse and cattle. *Cell and Tissue Research* **240**, 41–48.

TANIGUCHI K, MATSUSAKI Y, OGAWA K, SAITO T (1992) Fine structure of the vomeronasal organ in the common marmoset (*Callithrix jacchus*). *Folia Primatologica* **59**, 169–176.

VACCAREZZA OL, SEPICH LN, TRAMEZZANI JH (1981) The vomeronasal organ of the rat. *Journal of Anatomy* **132**, 167–185.

ZURI I, FISHELSON L, TERKEL J (1998) Morphology and cytology of the nasal cavity and vomeronasal organ in juvenile and adult blind mole rats (*Spalax ehrenbergi*). *Anatomical Record* **251**, 460–471.